

The C–H Stretching Features at 3.2–3.5 μm of Polycyclic Aromatic Hydrocarbons with Aliphatic Sidegroups

DRAFT: 2016.8.25.51

X.J. Yang^{1,2}, Aigen Li², R. Glaser³, and J.X. Zhong¹

ABSTRACT

The so-called “unidentified” infrared emission (UIE) features at 3.3, 6.2, 7.7, 8.6, and 11.3 μm are ubiquitously seen in a wide variety of astrophysical regions. The UIE features are characteristic of the stretching and bending vibrations of aromatic hydrocarbon materials, e.g., polycyclic aromatic hydrocarbon (PAH) molecules. The 3.3 μm aromatic C–H stretching feature is often accompanied by a weaker feature at 3.4 μm . The latter is generally thought to result from the C–H stretch of aliphatic groups attached to the aromatic systems. The ratio of the observed intensity of the 3.3 μm aromatic C–H feature to that of the 3.4 μm aliphatic C–H feature allows one to estimate the aliphatic fraction of the UIE carriers, provided that the intrinsic oscillator strengths of the 3.3 μm aromatic C–H stretch ($A_{3.3}$) and the 3.4 μm aliphatic C–H stretch ($A_{3.4}$) are known. While previous studies on the aliphatic fraction of the UIE carriers were mostly based on the $A_{3.4}/A_{3.3}$ ratios derived from the mono-methyl derivatives of small PAH molecules, in this work we employ density functional theory to compute the infrared vibrational spectra of PAH molecules with a wide range of sidegroups including ethyl, propyl, butyl, and several unsaturated alkyl chains, as well as all the isomers of dimethyl-substituted pyrene. We find that, except PAHs with unsaturated alkyl chains, the corresponding $A_{3.4}/A_{3.3}$ ratios are close to that of mono-methyl PAHs. This confirms the predominantly-aromatic nature of the UIE carriers previously inferred from the $A_{3.4}/A_{3.3}$ ratio derived from mono-methyl PAHs.

¹Department of Physics, Xiangtan University, 411105 Xiangtan, Hunan Province, China; xjyang@xtu.edu.cn, jxzhong@xtu.edu.cn

²Department of Physics and Astronomy, University of Missouri, Columbia, MO 65211, USA; lia@missouri.edu

³Department of Chemistry, University of Missouri, Columbia, MO 65211, USA; glaserr@missouri.edu

Subject headings: dust, extinction — ISM: lines and bands — ISM: molecules

1. Introduction

Over four decades ago, an important chapter of modern astrochemistry was opened by Gillett et al. (1973) who obtained from ground-based observations the $\sim 8\text{--}13\,\mu\text{m}$ spectra of two planetary nebulae (NGC 7027 and BD+30°3639) and reported the discovery of a broad emission feature at $11.3\,\mu\text{m}$. Two additional emission features peaking at 8.6 and $12.7\,\mu\text{m}$ were also prominent in their spectra. Since then other features have been observed, including the 6.2 and $7.7\,\mu\text{m}$ bands first discovered in NGC 7027 with airborne observations made with the *Kuiper Airborne Observatory* (Russell et al. 1977) and the $3.3\,\mu\text{m}$ band first discovered also in NGC 7027 through ground-based observations (Merrill et al. 1975). It had already become clear in the 1970s that these bands were part of a family of infrared (IR) emission features. Now, this family of emission features at 3.3 , 6.2 , 7.7 , 8.6 , 11.3 , and $12.7\,\mu\text{m}$ are ubiquitously seen in almost all celestial objects with associated gas and dust, including protoplanetary nebulae (PPNe), planetary nebulae (PNe), protoplanetary disks around young stars, reflection nebulae, HII regions, the Galactic IR cirrus, and external galaxies (see Tielens 2008). Collectively known as the “unidentified infrared emission” (UIE) bands, these features are a common characteristic of the interstellar medium (ISM) of the Milky Way and nearby galaxies as well as distant galaxies out to redshifts of $z \gtrsim 4$ (e.g., see Riechers et al. 2014). The “UIE” bands earned this name from the fact that the exact nature of their carriers remain unidentified, although many candidate materials have been proposed. Nevertheless, it is now generally accepted that these features are characteristic of the stretching and bending vibrations of some sorts of aromatic hydrocarbon materials (e.g., see Sellgren 2001, Peeters et al. 2002, Hudgins & Allamandola 2005)

Léger & Puget (1984) and Allamandola et al. (1985, 1989) attributed the UIE bands to gas-phase, free-flying polycyclic aromatic hydrocarbon (PAH) molecules. The PAH model attributes the UIE bands to the vibrational modes of PAHs with the $3.3\,\mu\text{m}$ feature assigned to C–H stretching modes, the $6.2\,\mu\text{m}$ and $7.7\,\mu\text{m}$ features to C–C stretching modes, the $8.6\,\mu\text{m}$ feature to C–H in-plane bending modes, and the $11.3\,\mu\text{m}$ feature to C–H out-of-plane bending modes. Alternatively, the UIE features have also been attributed to amorphous solids with a mixed aromatic/aliphatic composition like hydrogenated amorphous carbon (HAC; Jones et al. 1990), quenched carbonaceous composites (QCC; Sakata et al. 1990), coal or kerogen (Papoular et al. 1989).¹ As originally suggested by Duley & Williams (1981), all

¹The “MAON” model recently proposed by Kwok & Zhang (2011, 2013) also falls in this category, where

of these *solid* materials share the basic molecular structure of PAHs by containing arenes. They also contain aliphatic C–H bonds as well as other molecular structures often with other elements besides C and H.

One way to distinguish the PAH hypothesis from other models is to compare in the UIE carriers $N_{\text{C,aliph}}$, the number of carbon (C) atoms in aliphatic chains, with $N_{\text{C,arom}}$, the number of C atoms in aromatic rings. We define the *aliphatic fraction* of the UIE carriers as the fraction of C atoms in aliphatic chains. For $N_{\text{C,aliph}} \ll N_{\text{C,arom}}$, the aliphatic fraction is approximately $N_{\text{C,aliph}}/N_{\text{C,arom}}$, the ratio of the number of aliphatic C atoms to that of aromatic C atoms.

Aliphatic hydrocarbons can be probed through their C–H stretching vibrational band at $3.4\ \mu\text{m}$ (Pendleton & Allamandola 2002). In many interstellar and circumstellar environments the $3.3\ \mu\text{m}$ emission feature is indeed often accompanied by a weaker feature at $3.4\ \mu\text{m}$ (see Li & Draine 2012 and references therein). The $3.4\ \mu\text{m}$ emission feature itself is often also accompanied by several weak satellite features at 3.43 , 3.46 , 3.51 , and $3.56\ \mu\text{m}$ (e.g., see Geballe et al. 1985, Jourdain de Muizon et al. 1986, Joblin et al. 1996, Sloan et al. 1997, 2014, Kaneda et al. 2014, Mori et al. 2014, Hammonds et al. 2015, Ohsawa et al. 2016). We define $I_{3.4}$ and $I_{3.3}$ as the observed intensities of the $3.4\ \mu\text{m}$ and $3.3\ \mu\text{m}$ emission features, respectively. For those sources in which both the $3.4\ \mu\text{m}$ feature and the 3.43 , 3.46 , 3.51 , and $3.56\ \mu\text{m}$ satellite features have been detected, $I_{3.4}$, the observed intensity of the $3.4\ \mu\text{m}$ emission feature, also includes the contributions from the 3.43 , 3.46 , 3.51 , and $3.56\ \mu\text{m}$ satellite features. We also define $A_{3.4}$ and $A_{3.3}$ as the band strengths of the aliphatic and aromatic C–H bonds, respectively, on a per unit C–H bond basis. We note that $A_{3.4}$ includes the contributions from all the aliphatic C–H stretches in the ~ 3.4 – $3.6\ \mu\text{m}$ wavelength range. The ratio of the number of C atoms in aliphatic units to that in aromatic rings in the UIE carriers can be derived from $N_{\text{C,aliph}}/N_{\text{C,arom}} \approx 0.3 \times (I_{3.4}/I_{3.3}) \times (A_{3.3}/A_{3.4})$.²

As demonstrated by Li & Draine (2012) and Yang et al. (2013), one can place an upper limit of $\sim 2\%$ on the aliphatic fraction of the emitters of the UIE features by assigning the $3.4\ \mu\text{m}$ emission *exclusively* to aliphatic C–H (also see Rouillé et al. 2012, Steglich et al.

MAON stands for “*mixed aromatic/aliphatic organic nanoparticle*”.

²The factor “0.3” arises from the conversion of the number of C–H bonds ($N_{\text{C–H}}$) to the number of C atoms (N_{C}). For aliphatics, we take $N_{\text{C,aliph}} = 2.5N_{\text{C–H,aliph}}$ (i.e., one aliphatic C atom corresponds to 2.5 aliphatic C–H bonds) which is intermediate between methylene $-\text{CH}_2$ and methyl $-\text{CH}_3$. For aromatics, we take $N_{\text{C,arom}} = 0.75N_{\text{C–H,arom}}$ (i.e., one aromatic C atom corresponds to 0.75 aromatic C–H bond) which is intermediate between benzene C_6H_6 and coronene $\text{C}_{24}\text{H}_{12}$. When converting $N_{\text{C–H,aliph}}/N_{\text{C–H,arom}}$ to $N_{\text{C,aliph}}/N_{\text{C,arom}}$, a factor of $(0.75/2.5) = 0.3$ arises.

2013).³ However, these studies were mostly based on the $A_{3.4}/A_{3.3}$ ratios derived from the *mono-methyl* derivatives of small PAH molecules. In reality, the PAH molecules in space could harbor larger alkyl side chains such as ethyl, propyl, and butyl. Also, several alkyl side chains might be present in one PAH molecule. To explore the effects of *larger* alkyl side chains on $A_{3.4}/A_{3.3}$, in this work we employ density functional theory to compute the IR vibrational spectra of several PAH molecules with a wide range of sidegroups including ethyl, propyl, butyl, and several unsaturated alkyl chains. In §2 we briefly describe the computational methods. The structures of the molecules based on which we derive the band strengths of the aromatic and aliphatic C–H stretches are described in §3. We compute their IR vibrational spectra and report in §3 the calculated $A_{3.3}$ and $A_{3.4}$ oscillator strengths and their implications on the aliphatic fractions of the UIE carriers. In view of the fact that interstellar PAHs may have more than one alkyl side chain, we also consider in §3 the situation that there are two methyl groups attached to a PAH molecule, using pyrene as an example. We summarize our major results in §4.

2. Computational Methods

We use the Gaussian09 software (Frisch et al. 2009) to calculate the IR vibrational spectra for a range of aromatic molecules with a wide range of sidegroups (see Figure 1). We employ the hybrid density functional theoretical method (B3LYP) at the 6-311+G** level. The standard scaling is applied to the frequencies by employing a scale factor of ~ 0.9688 (Borowski 2012). Yang et al. (2013) have carried out computations for seven methylated PAH molecules with the B3LYP method in conjunction with a variety of basis sets. These basis sets, in order of increasing computational demand and accuracy, are 6-31G*, 6-31+G*, 6-311+G*, 6-311G**, 6-31+G**, 6-31++G**, 6-311+G**, 6-311++G**, 6-311+G(3df,3pd), and 6-311++G(3df,3pd). The second-order Møller-Plesset perturbation theory (MP2) is widely considered to be more accurate than B3LYP in computing band intensities (see Cramer et al. 2004). To examine the accuracy of the B3LYP method, Yang et al. (2013) have performed calculations with B3LYP and MP2, using the most extensive basis set 6-311++G(3df,3pd) for both methods. It is found that the results computed from B3LYP/6-311++G(3df,3pd) closely agree with that from MP2/6-311++G(3df,3pd). On the other hand, Yang et al. (2013) have also found that the results computed with the B3LYP method combined with

³This is indeed an *upper limit*: the actual aliphatic fraction could be lower since the aliphatic C–H stretch is not necessarily the sole contributor to the $3.4\mu\text{m}$ emission feature. This feature could also be caused by *anharmonicity* of the aromatic C–H stretch (Barker et al. 1987) and “*superhydrogenated*” PAHs whose edges contain excess H atoms (Bernstein et al. 1996, Sandford et al. 2013).

the four most sophisticated basis sets 6-311+G**, 6-311++G**, 6-311+G(3df,3pd), and 6-311++G(3df,3pd) essentially reach the convergence limit. The B3LYP/6-311+G** method therefore presents an excellent compromise between accuracy and computational demand. Therefore, in this work we adopt the B3LYP/6-311+G** method.

3. Results and Discussion

All of the molecules shown in Figure 1 are studied at the B3LYP/6-311+G** level. They cover a wide range of sidegroups, including ethyl ($-\text{CH}_2-\text{CH}_3$), propyl ($-\text{CH}_2-\text{CH}_2-\text{CH}_3$), butyl ($-\text{CH}_2-\text{CH}_2-\text{CH}_2-\text{CH}_3$), and several unsaturated alkyl groups and spacers ($-\text{CH}=\text{CH}_2$, $-\text{CH}=\text{CH}-$, $\text{C}=\text{CH}_2$, $\text{C}=\text{C}-\text{H}$). Most of the structures shown in Figure 1 are unremarkable and planar or very close to planar. Molecular models of the structures with significant twists around the (alkene)C–C(arene) bonds are shown in Figure 2 in two perspectives. The computed total energies and the thermochemical parameters are summarized in Table 1 for the minima.⁴

The vibrational frequencies and intensities for the aromatic and the aliphatic C–H stretching modes were computed. The computed intensities are shown in the top panel of Figure 3. We can see that the aliphatic C–H stretch band strength varies within a wide range. For ethyl, propyl and butyl, the values ($A_{3.4} \sim 25\text{--}30 \text{ km mol}^{-1}$) are generally consistent with methyl PAHs for which the aliphatic C–H stretch band strength has an average value (per aliphatic C–H bond) of $\langle A_{3.4} \rangle \approx 23.68 \text{ km mol}^{-1}$, with a standard deviation of $\sigma(A_{3.4}) \approx 2.48 \text{ km mol}^{-1}$ (see Yang et al. 2013). In contrast, the aliphatic C–H stretch strengths for the unsaturated alkyl chains ($-\text{CH}=\text{CH}_2$, $-\text{CH}=\text{CH}-$, $\text{C}=\text{CH}_2$, $\text{C}=\text{C}-\text{H}$) are much lower ($A_{3.4} \sim 5\text{--}15 \text{ km mol}^{-1}$). On the other hand, the aromatic C–H stretch band strength stays stable for all the groups, $A_{3.3} \sim 10\text{--}15 \text{ km mol}^{-1}$, which is also consistent with methyl PAHs for which the aromatic C–H stretch band strength has an average value (per aromatic C–H bond) of $\langle A_{3.3} \rangle \approx 14.03 \text{ km mol}^{-1}$, with a standard deviation of $\sigma(A_{3.3}) \approx 0.89 \text{ km mol}^{-1}$ (see Yang et al. 2013). Therefore, as shown in the bottom panel of Figure 3, we conclude that, with $\langle A_{3.4}/A_{3.3} \rangle \approx 1.97 \pm 0.12$, the $A_{3.4}/A_{3.3}$ ratios for PAHs with ethyl, propyl and butyl groups are close to that of methyl PAHs for which $\langle A_{3.4}/A_{3.3} \rangle \approx 1.76 \pm 0.21$ (see Yang et al. 2013). The $A_{3.4}/A_{3.3}$ ratios for PAHs with unsaturated alkyl chains ($\langle A_{3.4}/A_{3.3} \rangle \approx 0.80 \pm 0.24$) are lower by a factor of ~ 2 than that of

⁴A structure on the potential energy surface is a “stationary structure” if the net inter-atomic forces on each atom is acceptably close to zero. A “minimum” is a stationary structure for which a small distortion along any internal coordinate increases the energy (all curvatures are positive).

methyl PAHs.

With the ratios of the intrinsic band strengths $A_{3.4}/A_{3.3}$ computed, we can estimate the ratio of the number of C atoms in aliphatic units to that in aromatic rings in the UIE carriers from $N_{\text{C,aliph}}/N_{\text{C,arom}} \approx 0.3 \times (I_{3.4}/I_{3.3}) \times (A_{3.3}/A_{3.4})$. Yang et al. (2013) have compiled and analyzed the observed UIE spectra of 35 sources reported in the literature which display both the $3.3\ \mu\text{m}$ and $3.4\ \mu\text{m}$ C–H features. These sources include PPNe, PNe, reflection nebulae, HII regions, and photodissociated regions (PDRs). Yang et al. (2013) derived a median ratio of $\langle I_{3.4}/I_{3.3} \rangle \approx 0.12$, with the majority (31/35) of these sources having $I_{3.4}/I_{3.3} < 0.25$. With an average bond strength ratio of $A_{3.4}/A_{3.3} \approx 1.97$ derived here for PAHs with ethyl, propyl and butyl sidegroups, we obtain $N_{\text{C,aliph}}/N_{\text{C,arom}} \approx 0.018$. Even if we adopt $A_{3.4}/A_{3.3} \approx 0.80$ which is derived for PAHs with unsaturated alkyl chains, the aliphatic fraction is still only $N_{\text{C,aliph}}/N_{\text{C,arom}} \approx 0.045$. This suggests that, in agreement of the earlier findings of Li & Draine (2012) and Yang et al. (2013), the UIE emitters are predominantly aromatic. An aliphatic component is indeed present, as revealed by the $3.4\ \mu\text{m}$ C–H stretch, but it is only a very minor part of the UIE emitters.

More recently, Mori et al. (2014) obtained the $\sim 2.5\text{--}5.4\ \mu\text{m}$ emission spectra of 36 Galactic HII regions (or HII region-like objects) with the *Infrared Camera* (IRC) on board *AKARI* (Onaka et al. 2007). They determined the $3.4\ \mu\text{m}$ -to- $3.3\ \mu\text{m}$ band ratios $I_{3.4}/I_{3.3}$ in a uniform manner for all 36 HII regions and derived an average ratio of $\langle I_{3.4}/I_{3.3} \rangle \approx 0.25 \pm 0.10$ (T. Onaka 2016, private communication), which is ~ 2.1 times that of Yang et al. (2013; $\langle I_{3.4}/I_{3.3} \rangle \approx 0.12$). Again, the $3.4\ \mu\text{m}$ feature intensity $I_{3.4}$ includes the contributions from the weak satellite features at $\sim 3.4\text{--}3.5\ \mu\text{m}$. For the UIE carriers in these HII regions, the aliphatic content will be higher: $N_{\text{C,aliph}}/N_{\text{C,arom}} \approx 0.038$ if one adopts the $A_{3.4}/A_{3.3}$ ratios derived for PAHs with ethyl, propyl and butyl groups (i.e., $A_{3.4}/A_{3.3} \approx 1.97$), or $N_{\text{C,aliph}}/N_{\text{C,arom}} \approx 0.095$ if one adopts the $A_{3.4}/A_{3.3}$ ratios derived for PAHs with unsaturated alkyl chains (i.e., $A_{3.4}/A_{3.3} \approx 0.80$). Apparently, in either case the UIR carriers are still largely aromatic.

In view that several alkyl side chains might be present in one PAH molecule, we also consider the situation that there are two methyl groups attached to a PAH molecule, using pyrene as an example. We consider all possible isomers of dimethyl-substituted pyrene (see Figure 4). For dimethyl pyrenes, as shown in the top panel of Figure 5, the aliphatic C–H stretch band strength varies within $A_{3.4} \sim 18\text{--}27\ \text{km mol}^{-1}$, while these values for the aromatic C–H stretch are generally $A_{3.3} \sim 15\ \text{km mol}^{-1}$. The $A_{3.4}/A_{3.3}$ ratios, as shown in the bottom panel of Figure 5, vary from ~ 1.25 (Pyre110) to ~ 1.75 (Pyre27), with an average ratio of $\langle A_{3.4}/A_{3.3} \rangle \approx 1.57 \pm 0.13$, which is only $\sim 11\%$ lower than the mean ratio of $\langle A_{3.4}/A_{3.3} \rangle \approx 1.76$ computed from methyl PAHs (see Yang et al. 2013). With $\langle I_{3.4}/I_{3.3} \rangle \approx 0.12$ (Yang et al.

2013) or $\langle I_{3.4}/I_{3.3} \rangle \approx 0.25$ (Mori et al. 2014), we derive the aliphatic fraction of the UIE carriers from $\langle A_{3.4}/A_{3.3} \rangle \approx 1.57$ to be $N_{\text{C,aliph}}/N_{\text{C,arom}} \approx 0.023$ or $N_{\text{C,aliph}}/N_{\text{C,arom}} \approx 0.048$, respectively.

We also find that the methyl groups are essentially independent of each other. Noticeable effects on frequency and intensity only occur when several alkyl groups are placed in direct proximity. We note that for methyl PAHs the frequencies of the aliphatic C–H stretch are always smaller than $\sim 3000 \text{ cm}^{-1}$ and those for the aromatic C–H stretch are larger than $\sim 3000 \text{ cm}^{-1}$. The positions of the C–H stretches of simple alkenes and dienes coincide with the methyl signals of methyl-substituted PAHs. However, for $\text{CH}=\text{CH}_2$ and $\text{C}=\text{CH}_2$, one of the aliphatic C–H stretches falls at $\sim 3120 \text{ cm}^{-1}$ (i.e. in the “aromatic” region). For dimethyl pyrene Pyre45, there is also one frequency of the aliphatic C–H stretches that falls in the “aromatic” region ($\sim 3070 \text{ cm}^{-1}$).

We note that although the $3.4 \mu\text{m}$ *emission* feature is always much weaker than the $3.3 \mu\text{m}$ *emission* feature in most of the UIE sources (except several PPNe, see Geballe 1997, Tokunaga 1997), the opposite is seen in *absorption*. A broad *absorption* feature at $3.4 \mu\text{m}$, ubiquitously seen in the diffuse ISM of the Milky Way and external galaxies (see Sandford et al. 1991, 1995, Pendleton et al. 1994, Pendleton & Allamandola 2002), is generally attributed to *solid* aliphatic hydrocarbon dust. It is much broader than the $3.4 \mu\text{m}$ *emission* feature seen in the UIE sources (see Figure 1 in Li & Draine 2012), supporting the *bulk*, *solid* nature of the carriers of the $3.4 \mu\text{m}$ absorption feature. In some sources the $3.4 \mu\text{m}$ absorption feature is accompanied by a weaker $3.3 \mu\text{m}$ *absorption* feature (e.g., in the Galactic center source GCS 3, the $3.3 \mu\text{m}$ absorption feature is weaker than the predominant $3.4 \mu\text{m}$ feature by a factor of ~ 35 , see Chiar et al. 2000).

The $3.4 \mu\text{m}$ *absorption* feature of the diffuse ISM consists of three substructures at $\sim 3.38, 3.42, 3.48 \mu\text{m}$ (corresponding to $\sim 2955, 2925, 2870 \text{ cm}^{-1}$) which respectively arises from the asymmetric C–H stretches of the $-\text{CH}_3$ and $-\text{CH}_2-$ functional groups and the symmetric C–H stretch of the $-\text{CH}_3$ groups in saturated aliphatic hydrocarbon materials (see Pendleton & Allamandola 2002). Some sources also exhibit a subfeature at $\sim 3.51 \mu\text{m}$ (corresponding to $\sim 2850 \text{ cm}^{-1}$), attributed to the symmetric C–H stretch of the $-\text{CH}_2-$ groups. Pendleton & Allamandola (2002) derived an abundance ratio of $-\text{CH}_2-/-\text{CH}_3 \approx 2.5$, suggesting that the aliphatic hydrocarbon materials contain structures like $-\text{CH}_2-\text{CH}_2-\text{CH}_3$ and $-\text{CH}_2-\text{CH}_2-\text{CH}_2-\text{CH}_3$. However, it is more complicated to infer the possible structures of the aliphatic components of the UIE carriers from the relative strengths of the $3.4 \mu\text{m}$ emission feature and its associated satellite features at $3.43, 3.46, 3.51$ and $3.56 \mu\text{m}$. This is because the $3.4 \mu\text{m}$ emission feature and its satellite features could also be due to superhydrogenation (Bernstein et al. 1996, Sandford et al. 2013) and anharmonicity (Barker et al. 1987).

We stress that the carriers of the (stronger) 3.3 and (weaker) 3.4 μm *emission* features cannot be the same carriers of the (weaker) 3.3 and (stronger) 3.4 μm *absorption* features. While the former must be mostly aromatic, nano-sized and subject to stochastic heating by single photons (see Sellgren et al. 1983, Sellgren 1984, Puget et al. 1995, Draine & Li 2001), the latter are most likely sub- μm -sized and attain equilibrium temperatures in the ISM.

While it is widely accepted that the 3.4 μm *absorption* feature originates from aliphatic C–H stretch, it remains debated whether the major carbon-containing interstellar dust component is aliphatic or aromatic (see Furton et al. 1999, Greenberg & Li 1999, Draine 2007). Dartois et al. (2007) analyzed the $\sim 3.4\text{--}4.0\ \mu\text{m}$ spectrum of IRAS 08572+3915, a distant IR galaxy at redshift $z \sim 0.0583$, obtained with the *L*-band spectrometer of the *United Kingdom Infrared Telescope* (UKIRT). Let $\tau_{\text{arom}} \equiv \int \Delta\tau_{3.3}(\lambda) d\lambda$ be the optical depth ($\Delta\tau_{3.3}$) of the 3.3 μm aromatic C–H absorption feature integrated over wavelength, and $\tau_{\text{aliph}} \equiv \int \Delta\tau_{3.4}(\lambda) d\lambda$ be the optical depth ($\Delta\tau_{3.4}$) of the 3.4 μm aliphatic C–H absorption feature integrated over wavelength. From the 3.3 and 3.4 μm *absorption* features of IRAS 08572+3915, Dartois et al. (2007) determined $\tau_{\text{aliph}}/\tau_{\text{arom}} \approx 33.3$ and further derived $N_{\text{H,aliph}}/N_{\text{H,arom}} \gtrsim 12.5$ (which corresponds to $N_{\text{C,aliph}}/N_{\text{C,arom}} \gtrsim 5.0$), where $N_{\text{H,aliph}}$ and $N_{\text{H,arom}}$ are respectively the numbers of H atoms in aliphatic chains and in aromatic rings. Therefore, they argued that “*the bonding of hydrogen atoms in interstellar hydrogenated amorphous carbon is highly aliphatic*” (cf. Dartois et al. 2007).

More recently, Chiar et al. (2013) examined the $\sim 2.9\text{--}3.64\ \mu\text{m}$ spectrum of the diffuse ISM along the line of sight toward the Galactic center Quintuplet cluster obtained with the UKIRT *Cooled Grating Spectrometer* (CGS4). Taking a set of intrinsic strengths for the C–H stretches *larger* than that of Dartois et al. (2007) but comparable to that of this work,⁵ they derived $N_{\text{H,aliph}}/N_{\text{H,arom}} \approx 1.19$ (which corresponds to $N_{\text{C,aliph}}/N_{\text{C,arom}} \approx 0.48$) from $\tau_{\text{aliph}}/\tau_{\text{arom}} \approx 56.8$.

Nevertheless, taking into account the 6.2 μm aromatic C–C stretching feature observed both in the Galactic center Quintuplet sightline and in IRAS 08572+3915, Chiar et al. (2013) and Dartois et al. (2007) both concluded that the major carbon-containing interstellar dust component is largely *aromatic* (e.g., $N_{\text{C,aliph}}/N_{\text{C,arom}} \approx 0.087$ for the Galactic center Quintuplet region, see Chiar et al. 2013). Chiar et al. (2013) suggested that interstellar hydrocarbon dust may consist of a *large aromatic core* and a *thin aliphatic mantle* (but also see Jones et al. [2013] who argued for a *large aliphatic core* and a *thin aromatic mantle*

⁵The intrinsic strengths of the symmetric C–H stretches of the $-\text{CH}_2-$ and $-\text{CH}_3$ groups adopted by Chiar et al. (2013) are respectively ~ 7 and ~ 12 times as high as that of Dartois et al. (2007). The intrinsic strengths of the asymmetric C–H stretches of the $-\text{CH}_2-$ and $-\text{CH}_3$ groups as well as the aromatic C–H stretch adopted by Chiar et al. (2013) are all about twice as high as that of Dartois et al. (2007).

for sub- μm -sized hydrocarbon dust). If the carrier of the $3.4\ \mu\text{m}$ absorption feature seen in the diffuse ISM is indeed just a *thin* layer of aliphatic hydrocarbon material coated on a large aromatic core (instead of a *thick* mantle coated on an amorphous silicate core), the nondetection of the $3.4\ \mu\text{m}$ aliphatic C–H absorption polarization along the line of sight where the $9.7\ \mu\text{m}$ Si–O silicate feature polarization has been detected (Chiar et al. 2006) is no longer inconsistent with the core-mantle model, provided that the mantle coated on the silicate core is not aliphatic but aromatic. If the silicate core is surrounded by an aliphatic hydrocarbon mantle, one would expect the $3.4\ \mu\text{m}$ absorption feature to be polarized wherever the $9.7\ \mu\text{m}$ silicate feature is polarized (see Li & Greenberg 2002, Li et al. 2014).

4. Summary

The UIE carriers play an essential role in astrophysics as an absorber of the UV starlight, as an agent for photoelectrically heating the interstellar gas, and as a valid indicator of the cosmic star-formation rates. While the exact nature of the UIE carriers remains unknown, the ratios of the observed intensities of the $3.3\ \mu\text{m}$ aromatic C–H stretching emission feature ($I_{3.3}$) to that of the $3.4\ \mu\text{m}$ aliphatic C–H emission feature ($I_{3.4}$) could provide constraints on the chemical structures of the UIE carriers, i.e., are they mainly aromatic or largely aliphatic with a mixed aromatic/aliphatic structure? To this end, the knowledge of the intrinsic strengths (per chemical bond) of the $3.3\ \mu\text{m}$ aromatic C–H stretch ($A_{3.3}$) and the $3.4\ \mu\text{m}$ aliphatic C–H stretch ($A_{3.4}$) is required. While the intrinsic strengths of these C–H stretches were previously derived almost exclusively from the mono-methyl derivatives of small PAHs, it is the purpose of this work to derive $A_{3.4}/A_{3.3}$ based on extensive computations of the vibrational frequencies and intensities of a range of PAHs with side groups other than methyl using the hybrid density function theory (B3LYP) in conjunction with the 6-311+G** basis set. The major results are:

1. A wide range of sidegroups (other than methyl) have been considered, including ethyl ($-\text{CH}_2-\text{CH}_3$), propyl ($-\text{CH}_2-\text{CH}_2-\text{CH}_3$), butyl ($-\text{CH}_2-\text{CH}_2-\text{CH}_2-\text{CH}_3$) and several unsaturated alkyl chains ($-\text{CH}=\text{CH}_2$, $-\text{CH}=\text{CH}-$, $\text{C}=\text{CH}_2$, $\text{C}=\text{C}-\text{H}$). With $\langle A_{3.4}/A_{3.3} \rangle \approx 1.97$, the corresponding $A_{3.4}/A_{3.3}$ ratios are close to that of mono-methyl PAHs (for which $\langle A_{3.4}/A_{3.3} \rangle \approx 1.76$), except PAHs with unsaturated alkyl chains (for which, with an average ratio of $\langle A_{3.4}/A_{3.3} \rangle \approx 0.80$, the $A_{3.4}/A_{3.3}$ ratios could be lower by a factor of ~ 2).
2. Dimethyl pyrene is studied in the context that several alkyl side chains might be present in one PAH molecule. The $A_{3.4}/A_{3.3}$ ratio averaged over all the isomers of dimethyl-

substituted pyrene is ~ 1.57 , which is only $\sim 11\%$ lower than that of mono-methyl PAHs.

3. By attributing the $3.4\ \mu\text{m}$ feature exclusively to aliphatic C–H stretch (i.e., neglecting anharmonicity and superhydrogenation), we derive the fraction of C atoms in aliphatic form from $I_{3.4}/I_{3.3}$ and $A_{3.4}/A_{3.3}$, where $I_{3.4}/I_{3.3}$, the ratio of the power emitted from the $3.4\ \mu\text{m}$ feature to that from the $3.3\ \mu\text{m}$ feature, has a median ratio of $\langle I_{3.4}/I_{3.3} \rangle \approx 0.12$ for 35 astronomical sources (consisting of PPNe, PNe, reflection nebulae, HII regions, and PDRs) which exhibit both the $3.3\ \mu\text{m}$ and $3.4\ \mu\text{m}$ C–H features. With $A_{3.4}/A_{3.3} \approx 1.97$ for PAHs with ethyl, propyl and butyl sidegroups or $A_{3.4}/A_{3.3} \approx 1.57$ for dimethyl pyrene, the derived aliphatic fractions of the UIE carriers are $\sim 2\%$, in close agreement with that determined from methyl PAHs (for which $A_{3.4}/A_{3.3} \approx 1.76$). Even with $A_{3.4}/A_{3.3} \approx 0.80$ derived for PAHs with unsaturated alkyl chains, the aliphatic fraction is only $\sim 4.5\%$. We conclude that, in agreement of the earlier findings of Li & Draine (2012) and Yang et al. (2013), the UIE emitters are predominantly aromatic and the aliphatic component is only a very minor part of the UIE emitters. This conclusion remains valid for the UIE carriers in the 36 Galactic HII regions studied by Mori et al. (2014) for which $\langle I_{3.4}/I_{3.3} \rangle \approx 0.25 \pm 0.10$.

We thank Dr. Takashi Onaka and the anonymous referee for very helpful suggestions. AL and XJY are supported in part by NSFC 11473023, NSF AST-1311804, NNX13AE63G, and the University of Missouri Research Board. RG is supported in part by NSF-PRISM grant Mathematics and Life Sciences (0928053). Computations were performed using the high-performance computer resources of the University of Missouri Bioinformatics Consortium.

REFERENCES

- Allamandola, L. J. 1996, in *The Cosmic Dust Connection*, ed. J. M. Greenberg (Dordrecht: Kluwer), 81
- Allamandola, L. J., Tielens, A. G. G. M., & Barker, J. R. 1985, *ApJ*, 290, L25
- Allamandola, L. J., Tielens, A. G. G. M., & Barker, J. R. 1989, *ApJS*, 71, 733
- Barker, J. R., Allamandola, L. J., & Tielens, A.G.G.M. 1987, *ApJ*, 315, L61
- Bernstein, M. P., Sandford, S. A., & Allamandola, L.J. 1996, *ApJ*, 472, L127

- Borowski, P. 2012, *J. Phys. Chem. A*, 116, 3866
- Chiar, J.E., Tielens, A.G.G.M., Whittet, D.C.B., et al. 2000, *ApJ*, 537, 749
- Chiar, J. E., Adamson, A. J., Whittet, D. C. B., et al. 2006, *ApJ*, 651, 268
- Chiar, J. E., Tielens, A. G. G. M., Adamson, A. J., & Ricca, A. 2013, *ApJ*, 770, 78
- Cramer, C. J. 2004, *Essentials of Computational Chemistry: Theories and Models*, Wiley
- Dartois, E., & Muñoz-Caro, G. M. 2007, *A&A*, 476, 1235
- d'Hendecourt, L. B., & Allamandola, L.J. 1986, *A&AS*, 64, 453
- Draine, B. T. 2006, in *Pre-Solar Grains as Astrophysical Tools*, 26th meeting of the IAU, Joint Discussion 11 (21 August 2006, Prague, Czech Republic)
- Draine, B.T., & Li, A. 2001, *ApJ*, 551, 807
- Duley, W. W., & Williams, D. A. 1981, *MNRAS*, 196, 269
- Frisch, M. J., Trucks, G. W., Schlegel, H. B., et al. 2009, *Gaussian 09*, Revision B01, Gaussian, Inc., Wallingford CT
- Furton, D. G., Laiho, J. W., & Witt, A. N. 1999, *ApJ*, 526, 752
- Geballe, T.R. 1997, in *From Stardust to Planetesimals*, ASP Conf. Ser. 122, ed. Y. J. Pendleton & A. G. G. M. Tielens (San Francisco: ASP), 119
- Geballe, T.R., Lacy, J.H., Persson, S.E., McGregor, P.J., & Soifer, B.T. 1985, *ApJ*, 292, 500
- Gillett, F. C., Forrest, W. J., & Merrill, K. M. 1973, *ApJ*, 183, 87
- Greenberg, J.M., & Li, A. 1999, *Adv. Space Res.*, 24, 497
- Hammonds, M., Mori, T., Usui, F., & Onaka, T. 2015, *Planet. Space Sci.*, 116, 73
- Hudgins, D. M., & Allamandola, L. J. 2005, in *IAU Symp. 231, Astrochemistry: Recent Successes and Current Challenges*, ed. D. C. Lis, G. A. Blake, & E. Herbst (Cambridge: Cambridge Univ. Press), 443
- Joblin, C., Tielens, A.G.G.M., Allamandola, L.J., & Geballe, T.R. 1996, *ApJ*, 458, 610
- Jones, A. P., Duley, W. W., & Williams, D. A. 1990, *QJRAS*, 31, 567
- Jones, A. P., Fanciullo, L., Köhler, M., et al. 2013, *A&A*, 558, A62

- Jourdain de Muizon, M., Geballe, T.R., d'Hendecourt, L.B., & Baas, F. 1986, *ApJ*, 306, L105
- Kaneda, H., Ishihara, D., Kobata, K., et al. 2014, *Planet. Space Sci.*, 100, 6
- Kwok, S., & Zhang, Y. 2011, *Nature*, 479, 80
- Léger, A., & Puget, J. 1984, *A&A*, 137, L5
- Li, A., & Greenberg, J. M. 2002, *ApJ*, 577, 789
- Li, A., & Draine, B. T. 2012, *ApJ*, 760, L35
- Li, Q., Liang, S. L., & Li, A. 2014, *MNRAS*, 440, L56
- Merrill, K. M., Soifer, B. T., & Russell, R. W. 1975, *ApJ*, 200, L37
- Mori, T. I., Onaka, T., Sakon, I., et al. 2014, *ApJ*, 784, 53
- Ohsawa, R., Onaka, T., Sakon, I., Matsuura, M., & Kaneda, H. 2016, *AJ*, 151, 93
- Onaka, T., Matsuhara, H., Wada, T., et al. 2007, *PASJ*, 59, S401
- Papoular, R., Conrad, J., Giuliano, M., Kister, J., & Mille, G. 1989, *A&A*, 217, 204
- Peeters, E., Hony, S., Van Kerckhoven, C., Tielens, A. G. G. M., Allamandola, L. J., Hudgins, D. M., & Bauschlicher, C. W. 2002, *A&A*, 390, 1089
- Pendleton, Y. J., & Allamandola, L. J. 2002, *ApJS*, 138, 75
- Pendleton, Y. J., Sandford, S. A., Allamandola, L. J., Tielens, A. G. G. M., & Sellgren, K. 1994, *ApJ*, 437, 683
- Pilleri, P., Joblin, C., Boulanger, F., & Onaka, T. 2015, *A&A*, 577, A16
- Puget, J.L., Léger, A., & d'Hendecourt, L. 1995, *A&A*, 293, 559
- Riechers, D. A., Pope, A., Daddi, E., et al. 2014, *ApJ*, 796, 84
- Rouillé, G., Steglich, M., Carpentier, Y., et al. 2012, *ApJ*, 752, 25
- Russell, R. W., Soifer, B. T., & Willner, S. P. 1977, *ApJ*, 217, L149
- Sakata, A., Wada, S., Onaka, T., & Tokunaga, A. T. 1990, *ApJS*, 353, 543
- Sandford, S. A., Bernstein, M. P., & Materese, C. K. 2013, *ApJS*, 205, 8

- Sandford, S. A., Allamandola, L. J., Tielens, A. G. G. M., et al. 1991, *ApJ*, 371, 607
- Sandford, S. A., Pendleton, Y. J., & Allamandola, L. J. 1995, *ApJ*, 440, 697
- Sellgren, K., Werner, M. W., & Dinerstein, H. L. 1983, *ApJ*, 271, L13
- Sellgren, K. 1984, *ApJ*, 277, 623
- Sellgren, K. 2001, *Spectrochim. Acta*, A57, 627
- Sloan, G.C., Bregman, J.D., Geballe, T.R., Allamandola, L.J., & Woodward, C.E. 1997, *ApJ*, 474, 735
- Sloan, G. C., Jura, M., Duley, W. W., et al. 2007, *ApJ*, 664, 1144
- Sloan, G. C., Lagadec, E., Zijlstra, A. A., et al. 2014, *ApJ*, 791, 28
- Steglich, M., Jäger, C., Huisken, F., et al. 2013, *ApJS*, 208, 26
- Tielens, A. G. G. M. 2008, *ARA&A*, 46, 289
- Tokunaga, A.T. 1997, in *ASP Conf. Ser. 124, Diffuse Infrared Radiation and the IRTS*, ed. H. Okuda, T. Matsumoto, & T. Roellig (San Francisco, CA: ASP), 149
- Yang, X. J., Glaser, R., Li, A., & Zhong, J. X. 2013, *ApJ*, 776, 110

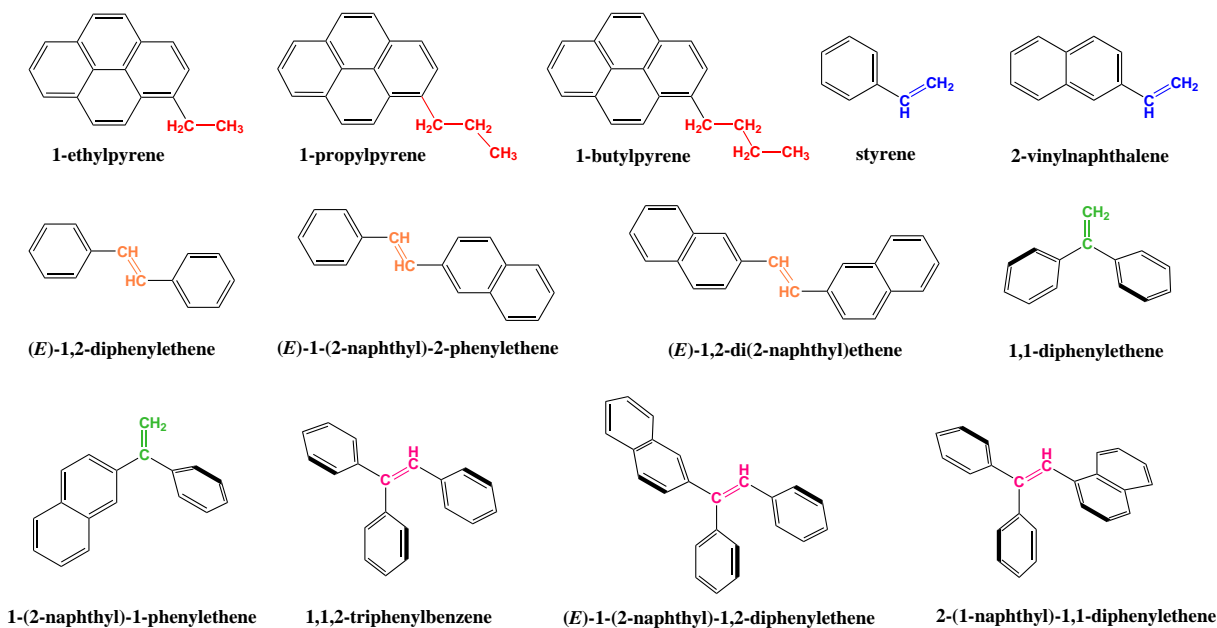


Fig. 1.— Effects of the nature of the alkyl group on the $A_{3.4}/A_{3.3}$ ratio were examined for 1-(n-alkyl)pyrene by consideration of ethyl ($-\text{CH}_2-\text{CH}_3$), propyl ($-\text{CH}_2-\text{CH}_2-\text{CH}_3$), and butyl ($-\text{CH}_2-\text{CH}_2-\text{CH}_2-\text{CH}_3$). Effects of olefinic C–H bonds on $A_{3.4}/A_{3.3}$ were examined for a number of vinyl-substituted systems ($-\text{CH}=\text{CH}_2$) and for a number of systems with ethene spacers ($-\text{CH}=\text{CH}-$, $\text{C}=\text{CH}_2$, $\text{CH}=\text{C}-\text{H}$).

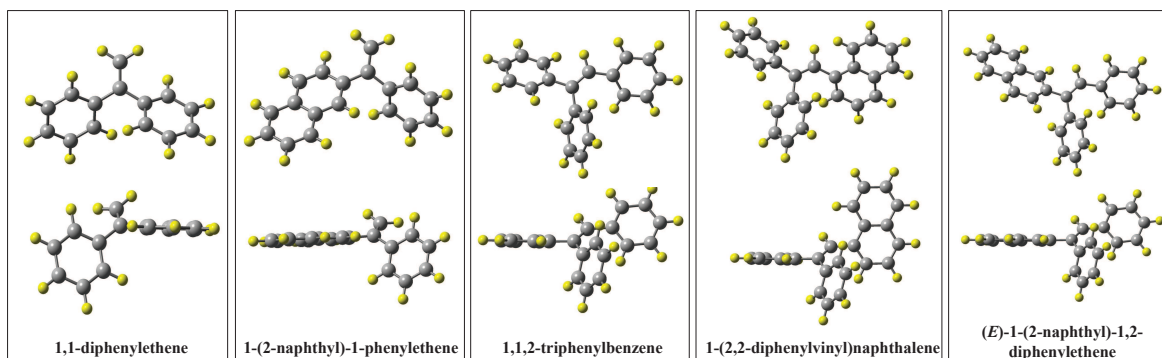


Fig. 2.— Optimized structures of phenyl- and naphthyl-substituted ethene. H atoms are shown in yellow and C atoms in grey. All structures are minima.

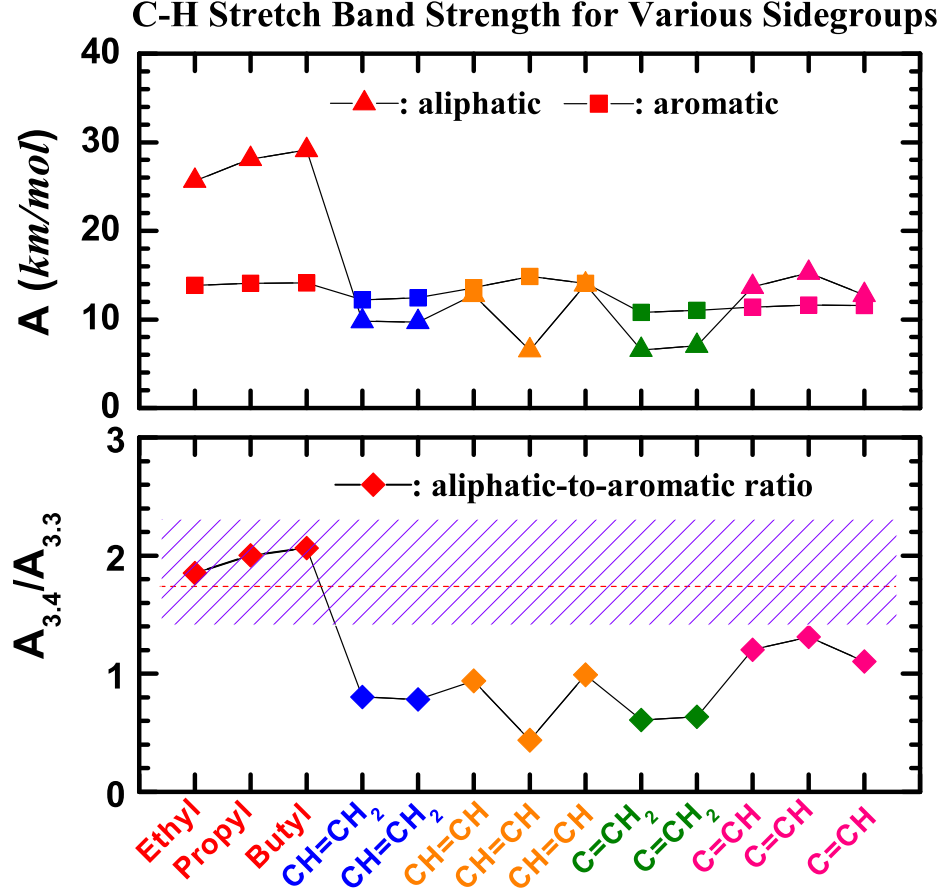


Fig. 3.— Band-strengths as determined with the B3LYP/6-311+G** method for PAHs with sidegroups other than methyl: ethyl ($-\text{CH}_2-\text{CH}_3$), propyl ($-\text{CH}_2-\text{CH}_2-\text{CH}_3$), butyl ($-\text{CH}_2-\text{CH}_2-\text{CH}_2-\text{CH}_3$), and unsaturated alkyl chains ($-\text{CH}=\text{CH}_2$, $-\text{CH}=\text{CH}-$, $\text{C}=\text{CH}_2$, $\text{C}=\text{C}-\text{H}$). The shaded region shows the range of $1.4 < A_{3.4}/A_{3.3} < 2.3$ derived for mono-methyl PAHs which has a mean value of $\langle A_{3.4}/A_{3.3} \rangle \approx 1.76$ plotted here as a red dashed line (see Yang et al. 2013).

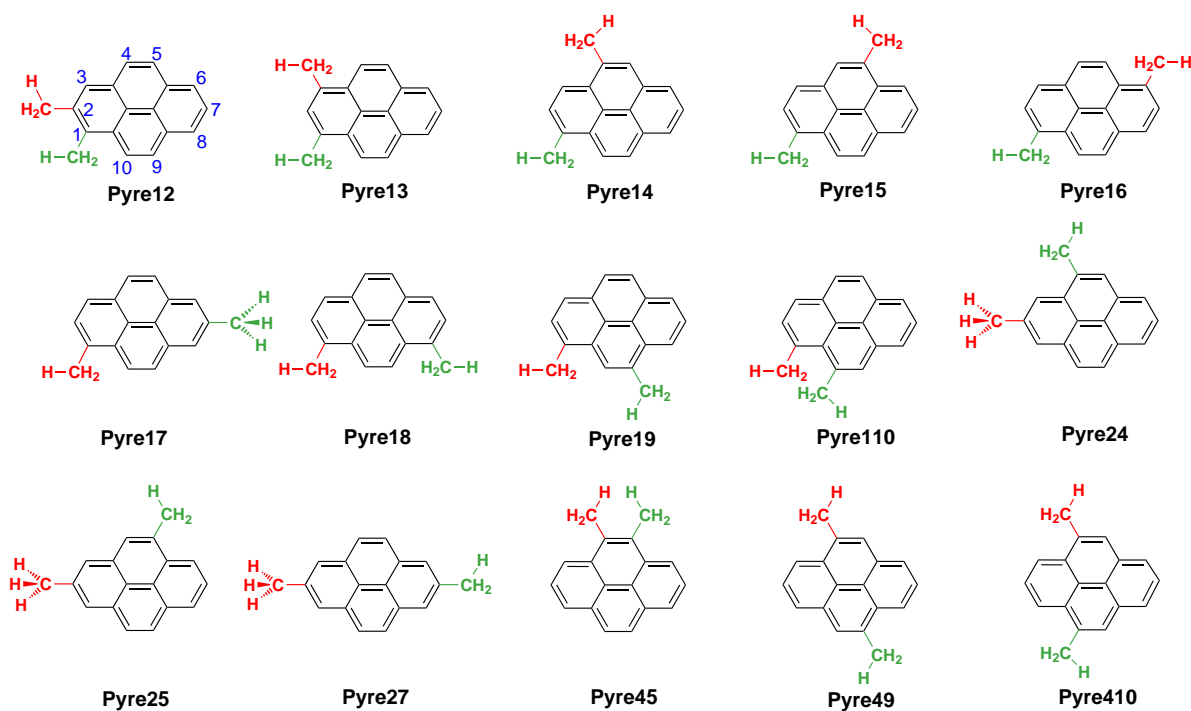


Fig. 4.— Structures of all isomers of dimethylpyrene. The naming method follows the standard *International Union of Pure and Applied Chemistry* (IUPAC) numbering scheme. We use the first four letters of the molecule to refer to it and attach the position number of the location of the methyl group: “Pyre” stands for pyrene, and the digits specify the locations of the attached methyl groups (e.g., “Pyre110” means the two methyl groups are attached at positions 1 and 10).

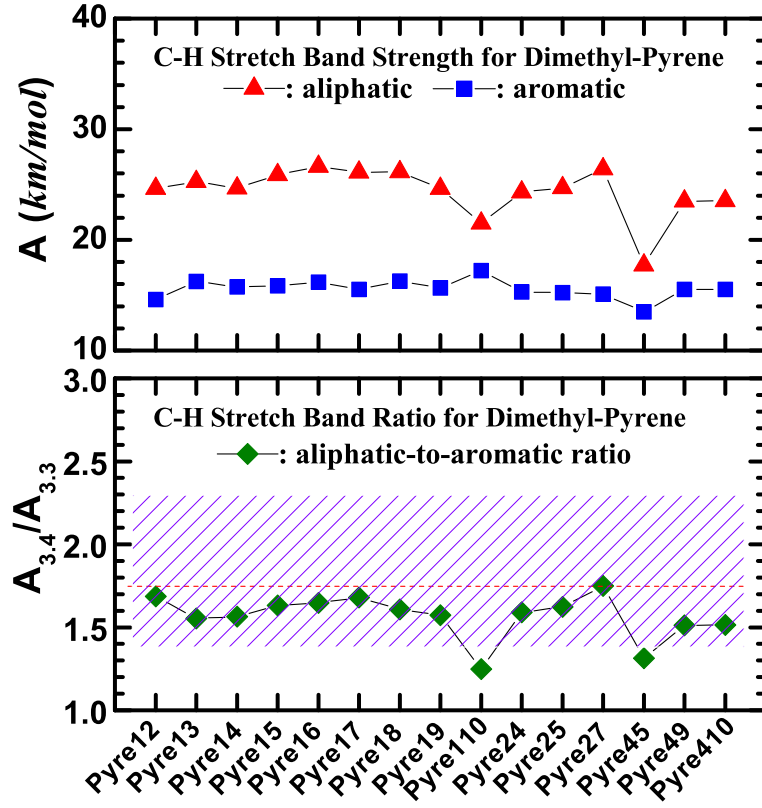


Fig. 5.— Band-strength as determined with the B3LYP/6-311+G** method for all the isomers of dimethyl pyrene. The shaded region shows the range of $1.4 < A_{3.4}/A_{3.3} < 2.3$ derived for mono-methyl PAHs which has a mean value of $\langle A_{3.4}/A_{3.3} \rangle \approx 1.76$ (red dashed line; see Yang et al. 2013).

Table 1: Computed Total Energies and Thermochemical Parameters for the Molecules Shown in Figure 1 at the B3LYP/6-311+G** Level.

Compound	E_{tot}^a	VZPE ^b	TE ^c	S^d	ν_1^e	ν_2^e	μ^f
1-ethylpyrene	-694.563690	164.68	172.86	111.66	49.40	99.48	0.6960
1-propylpyrene	-733.887721	182.33	191.44	119.15	40.80	89.70	0.7423
1-butylpyrene	-773.212086	200.09	210.07	126.68	30.03	72.90	0.7933
styrene	-309.730792	83.30	87.59	83.88	22.17	205.09	0.2065
2-vinylnaphthalene	-463.409350	112.66	118.47	94.45	57.54	132.81	0.2748
(E)-1,2-diphenylethene	-540.846680	134.22	141.34	109.43	13.17	57.63	0.0000
(E)-1-(2-naphthyl)-2-phenylethene	-694.525418	163.54	172.24	120.20	22.42	45.62	0.0489
(E)-1,2-di(2-naphthyl)ethene	-848.202613	192.60	202.99	135.13	9.80	31.38	0.1256
1,1-diphenylethene	-540.839566	134.16	141.11	105.16	40.25	60.61	0.2926
1-(2-naphthyl)-1-phenylethene	-694.517262	163.35	171.95	118.19	32.50	49.65	0.3264
1,1,2-triphenylbenzene	-771.949489	184.92	194.84	130.27	30.52	42.19	0.3446
(E)-1-(2-naphthyl)-1,2-diphenylethene	-925.627411	214.08	225.67	143.17	28.83	37.95	0.3844
2-(1-naphthyl)-1,1-diphenylethene	-925.625007	214.17	225.73	142.78	23.86	37.53	0.3252

^a Total energies in atomic units.

^b Vibrational zero-point energies (VZPE) in kcal mol⁻¹.

^c Thermal energies (TE) in kcal mol⁻¹.

^d Molecular entropies (S) in cal mol⁻¹ K⁻¹.

^e The lowest vibrational modes ν_1 and ν_2 in cm⁻¹.

^f Dipole moment in Debye.

Table 2: Computed Total Energies and Thermochemical Parameters for All the Isomers of Dimethylpyrene Shown in Figure 4 at B3LYP/6-311+G**.

Compound	E_{tot}	VZPE	TE	S	ν_1	ν_2	μ
Pyre12	-694.404435	165.41	173.78	112.18	74.32	89.80	0.7983
Pyre13	-694.406226	165.39	173.77	110.68	87.00	87.07	0.5684
Pyre14	-694.407131	165.47	173.81	111.63	81.42	105.91	0.4788
Pyre15	-694.407075	165.49	173.82	111.57	86.33	89.70	0.0852
Pyre16	-694.406142	165.42	173.78	110.45	72.15	111.02	0.0001
Pyre17	-694.407577	165.04	173.61	115.48	33.38	68.01	0.3259
Pyre18	-694.406206	165.38	173.76	112.02	83.93	94.45	0.5851
Pyre19	-694.406998	165.50	173.82	111.45	73.06	113.95	0.5783
Pyre110	-694.396367	165.75	174.01	112.73	28.02	100.75	0.7623
Pyre24	-694.408443	165.15	173.67	114.77	36.84	69.11	0.7083
Pyre25	-694.408459	165.18	173.69	114.75	35.29	73.52	0.3881
Pyre27	-694.408977	164.77	173.51	117.35	29.34	36.07	0.0000
Pyre45	-694.400927	165.72	174.03	110.48	74.28	76.98	0.5827
Pyre49	-694.408023	165.53	173.83	109.86	73.49	119.07	0.0002
Pyre410	-694.407838	165.56	173.85	111.16	75.60	121.61	0.4010